# The Effect of Using Finite-Width Electrostatic Gates in Time-of-Flight Measurements for Colloid Thrusters*

Paulo Lozano and Manuel Martínez-Sánchez
Massachusetts Institute of Technology
Room 37-438
70 Vassar St
Cambridge, MA 02139
617-253-7485
plozano@mit.edu and mmart@mit.edu

IEPC-01-286

**In this paper we present the latest results in our time-of-flight (TOF) spectrometer program for analyzing colloid thruster plumes. Previous results, particularly in relatively slow droplet beams, showed an inconsistency between the measurements and the theory of electrosprays operating in the cone-jet mode. This inconsistency was due to the type of electrostatic gating used. A mathematical analysis is developed in which the effect of Finite-Width gates is described and used to recover as much information as possible from the data. This method could be extended to other analytical systems that require the use of electrostatic gates.**

## Introduction

Colloid thrusters, working on the principle of electrostatic extraction and acceleration of highly charged liquid droplets and/or ions, are one of several microthruster technologies currently receiving attention for applications ranging from main propulsion of microsatellites to high-precision altitude control and station keeping of constellation members. An introduction to the technology and a review of its earlier implementation as a mainline propulsion concept (in the 1960's and 1970's) can be found in [1].

One of the most useful techniques to characterize these plumes is by the use of Time-of-Flight (TOF) spectrometry in which a beam of charged particles is forced to drift towards a detector in a pulse mode. The time of travel from the emitter to the detector gives enough information to estimate the specific charge of the different particles that compose the beam if its mean energy value and spread are known. Specific charge and beam composition are very important to determine the performance of a Colloid Thruster as the propulsive efficiency and specific impulse depend directly on those parameters.

A common part of all TOF spectrometers is at least one electrostatic gate, which allows or stops the flow of particles towards the detector. The gating mechanism introduces electric fields that could modify the energy level of the particles. This is an important topic for mass spectrometer specialists, who have created gates that present symmetric potentials upstream and downstream along the particle's path when closed and therefore are almost free from these effects. Some of these devices are constructed from very thin conducting filaments closely spaced together having alternating positive and negative potentials (interleaved combs). The most elementary type of symmetric gate would be a set of parallel plates.

Interleaved comb gates may be unsuitable for colloid experimentation since droplets could deposit in the filaments, possibly short-circuiting them. If finite-width devices need to be used, gate effects that would modify the measurements can be expected. In this paper we discuss such effects and elaborate on a model to describe them and to determine to what extent useful information can be recovered from affected data.

## Colloid Plumes: Ion-Droplet Regime

The physics of colloidal electrosprays, as presently understood [1], offers the possibility of achieving high specific impulses (>1000 s.) with pure droplets

* Presented as Paper IEPC-01-286 at the 27th International Electric Propulsion Conference, Pasadena, CA, 15-19 October, 2001.

only, but only at fairly high acceleration voltages. This is because, even with ionic conductivities as high as several Si/m, the droplet specific charge achievable is limited to roughly that which would result from all the ions of one polarity in the initial solution, for a droplet at the electrostatic breakup limit (Rayleigh limit). On the other hand, it is known that, under some conditions, pure ions can be extracted from liquids (FEEP being the extreme case of liquid metals). So far only strong acids have been shown to yield ions with no accompanying droplets [2], but there are preliminary indications [3] that ionic liquids may in fact be made to operate in the pure ion mode as well. For ions with single charge and molecular mass in the range of 100-400 g/mole, voltages of the order of 1-3kV, as required to overcome surface tension, tend to yield very high specific impulses, generally above the optimum range.

An alternative, which we are pursuing, is the use of mixed streams of ions and droplets in order to tailor the specific impulse to the mission requirements. The efficiency penalty due to the stream's polydispersity [1] may be acceptable for many missions. To characterize the colloid plumes in this regime we require to perform TOF measurements of both species.

Most TOF spectrometers are specifically designed to detect ionic species, not droplets. In most cases, they make use of micro channel plates (MCP) as the detector element. The extreme sensitivity of MCPs makes them ideal for species identification. They however, give no direct indication of particle fluxes. In addition, it is not clear how the flow of droplets would affect the functioning of a MCP since there would also be unavoidable liquid deposition over the detector surfaces. An alternative to the use of a MCP is to substitute it by a sensitive electrometer capable of measuring extremely low current levels.

We have designed a TOF apparatus that separates droplets and ions by performing measurements for each possible charged species present in the beam, allowing one to construct the spectrum. This is accomplished by the use of two electrostatic finite-width gates, one at the emission point and one near the detector. The gates open and close in such a way that they allow a single species through the TOF path for a given time during each cycle until the electrometer picks up enough charges to determine the flux. The delay between the pulses is then modified to detect the next beam component. The process is repeated until the spectrum is completed. A comprehensive description of the custom designed TOF spectrometer can be found in [4].

Preliminary measurements done with this system [4] showed that the principle works, but there was an inconsistency between the observations and what can be expected theoretically for the fluid used. As it turns out, such discrepancies appear to be related to the type of electrostatic gate installed in the experimental setup. It was found that the droplet velocities measured were larger than expected; somehow the closing of the gates added energy to the beam, increasing its speed.

## Electrostatic Gate Modeling

As discussed above, the electrostatic finite-width gates used in our experiments present a potential barrier that could be either open or closed for a particle to reach the current collector or be stopped and bounced back. The simplest model (which could be also the correct one in a charge-free spatial region) of the gate is a linear barrier grounded at its extremes as shown in figure 1. The parameters that completely describe this barrier are the position of the maximum voltage ($x_m$), the position of the second ground ($x_\infty$), the maximum voltage ($\phi_m$) and the time ($T$) during which the gate voltage goes to zero and particles are allowed to go through it. Shown also is the potential level ($V$) of the particle beam. It is clear that, since $V < \phi_m$, all particles are stopped when the barrier is up.

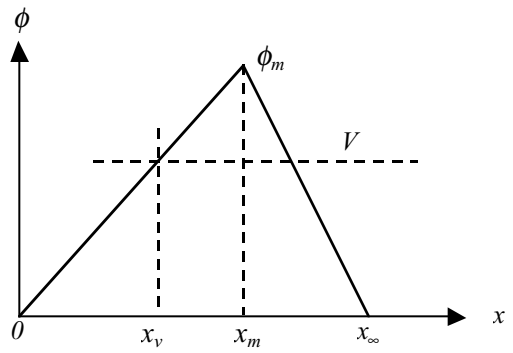


Figure 1 — Electrostatic gate potential barrier

In our experiments, the barrier is normally closed and opens only for a small time $T$. Defining $x_0$ as the position of a particle at the time when the barrier is

opened, the position of the particle at the moment when the barrier closes is

$$x_T = x_0 + T\sqrt{2\tfrac{q}{m}\left(V - \phi_m \frac{x_0}{x_m}\right)} \quad \text{for} \quad x_0 > 0$$
$$x_T = x_0 + T\sqrt{2\tfrac{q}{m}V} \quad \text{for} \quad x_0 < 0 \tag{1}$$

If the particle has enough energy to pass the peak potential of the barrier by the time it closes, it will in general leave with a different energy than the one it had before entering the barrier influence zone. This is evident since the fields generated by the potential distribution are axially directed and they accelerate or decelerate charged particles depending on their positions.

The different regions that share an energy level in the exit plane are shown in table 1 in terms of the non-dimensional parameters:

$$\xi_0 = \frac{x_0}{x_m} \quad \xi_\infty = \frac{x_\infty}{x_m} \quad \alpha_v = \frac{V}{\phi_m}$$
$$\alpha_T = \frac{q}{m}\phi_m (T/x_m)^2 \tag{2}$$

Table 1 — Regions with different energy characteristics

| Region | $\xi_0$ | $\xi_T$ |
|---|---|---|
| A1 | $\xi_0 < 0$ | $\xi_T < 0$ |
| A2 | | $0 < \xi_T < 1$ |
| A3 | | $1 < \xi_T < \xi_\infty$ |
| A4 | | $\xi_T > \xi_\infty$ |
| B1 | $\xi_0 > 0$ | $\xi_0 < \xi_T < 1$ |
| B2 | | $1 < \xi_T < \xi_\infty$ |
| B3 | | $\xi_T > \xi_\infty$ |

For each of these regions the non-dimensional energy gain (or loss) is given by

$$\Delta\varepsilon = \frac{(\phi_T - \phi_0)}{V} \tag{3}$$

Table 2 shows the energy level for each region and whether it contains particles that pass or bounce from the potential barrier.

Table 2 — Energy change of particles

| R | $\Delta\varepsilon$ | Pass the barrier? |
|---|---|---|
| A1 | 0 | No |
| A2 | $\frac{\xi_0 + \sqrt{2\alpha_v\alpha_T}}{\alpha_v}$ | If $\xi_0$ is larger than $1-\alpha_v-\sqrt{2\alpha_v\alpha_T}$ |
| A3 | $\frac{\xi_\infty - \xi_0 - \sqrt{2\alpha_v\alpha_T}}{\alpha_v(\xi_\infty - 1)}$ | Yes |
| A4 | 0 | Yes |
| B1 | $\frac{\sqrt{2\alpha_T(\alpha_v - \xi_0)}}{\alpha_v}$ | If $\xi_0$ is less than $\alpha_v - \frac{(1-\alpha_v)^2}{2\alpha_T}$ |
| B2 | $\frac{\xi_\infty - \xi_0 - \sqrt{2\alpha_T(\alpha_v - \xi_0)}}{\alpha_v(\xi_\infty - 1)} - \frac{\xi_0}{\alpha_v}$ | Yes |
| B3 | $-\frac{\xi_0}{\alpha_v}$ | Yes |

The velocity at which particles leave the gate is then

$$v_\infty = v_s\sqrt{1+\Delta\varepsilon} \quad \text{with} \quad v_s = \sqrt{2\tfrac{q}{m}V} \tag{4}$$

$v_s$ being the source particle velocity.

Plotted in figure 2 are lines of $v_\infty / v_s$ with respect to the initial position $\xi_0$. Three cases are shown. In the first one (q/m = 127 C/kg), all particles exit the gate with a velocity $v_\infty > v_s$. The net effect that would be expected is a shift and broadening of the measured spectrum for these conditions. In the second and third cases the region A4 appears as the region in which the velocity remains unchanged. For these cases a fraction of the particles leave the gate with velocities lower than the source velocity. For these plots the following parameters were used: $T$ = 30μsec, $x_m$ = 10mm, $x_\infty$ = 15mm, $V$ = 700V and $\phi_m$ = 950V.

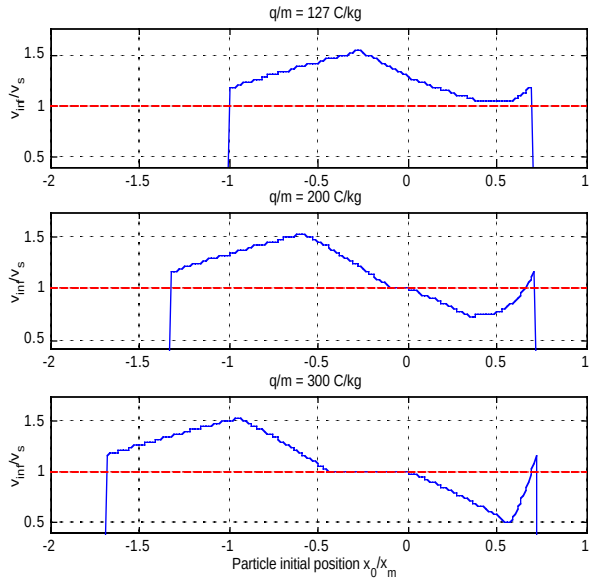


Figure 2 — Velocity maps for different specific charges

**Data Analysis and Recovery**

There are two important applications that can result from the analysis of the ideal finite-width electrostatic gate. The first is a detailed understanding of the effects that such gates have on experimental measurements and the second is the possibility of recovering useful information from degraded data.

If we write the probability density function for having a velocity between $v_\infty$ and $v_\infty + dv_\infty$ as depending on the individual probability density functions $f_{x_0}(x_0)$ and $f_{q/m}(q/m)$ with $q/m = q/m(v_\infty, x_0)$ we have

$$f_{v_\infty} dv_\infty = \int_{-\infty}^{\infty} f_{x_0}(x_0) dx_0 \, f_{q/m}\left(q/m(v_\infty, x_0)\right) d\,q/m \qquad (5)$$

and for a line of constant $x_0$

$$dv_\infty = \frac{\partial v_\infty}{\partial x_0} dx_0 + \frac{\partial v_\infty}{\partial q/m} d\,q/m = \left(\frac{\partial v_\infty}{\partial q/m}\right)_{x_0} d\,q/m \qquad (6)$$

We obtain for the velocity distribution function

$$f_{v_\infty}(v_\infty) = \int_{-\infty}^{\infty} f_{q/m}(q/m) \, f_{x_0}\left[x_0(v_\infty, q/m)\right] \frac{d\,q/m}{\left(\left|\frac{\partial v_\infty}{\partial x_0}\right|\right)_{x_0}(v_\infty, q/m)} \qquad (7)$$

Defining $n(x_0)$ and $v(x_0)$ as the number of particles per unit length and particle velocity at $x_0$, then the fraction of passing particles per unit length $dx_0$ in the interval between $x_0$ and $x_0 + dx_0$ is

$$f_{x_0}(x_0) = \frac{n(x_0)}{\int_{x_0\,\min}^{x_0\,\max} n(x_0') dx_0'} \qquad (8)$$

where $[x_{0\min}, x_{0\max}]$ defines the interval in which particles pass the barrier. Since the particle flux $(\Gamma)$ must be conserved

$$\Gamma = nv = n(x_0)v(x_0) \qquad (9)$$

Substituting (9) into (8) and using tables 1 and 2, the passing particle fraction is

$$f_{x_0}(x_0) = Q^{-1} \begin{cases} 1 & \text{for} \quad \xi_0 < 0 \\ (1 - \xi_0/\alpha_v)^{-1/2} & \text{for} \quad \xi_0 > 0 \end{cases} \qquad (10)$$

in which the coefficient $Q$ is given by

$$Q = x_m\left(\alpha_v + \sqrt{2\alpha_v\alpha_T} - 1\right)\left(1 + \sqrt{2\alpha_v/\alpha_T}\right) \qquad (11)$$

Equations (1-4, 10-11) and tables 1 and 2 can be used to compute the elements of (7) for a given set of physical parameters, with the exception of those particles contained in region A4 for which a special treatment is required.

Since all particles in region A4 pass the barrier without energy change, then the function $f_{x_0}(x_0)$ is a constant and the partial derivative in eq. (7) is zero. This means that

$$f_{x_0}\left[x_0(v_\infty)\right]\left(\frac{\partial v_\infty}{\partial x_0}\right)^{-1} \to \infty \qquad (12)$$

and this quantity is a Dirac delta whose contribution can be added to the rest of the terms in eq. (7). The delta in (12) can be written as

$$f_{x_0}\left[x_0(v_\infty)\right]\left(\frac{\partial v_\infty}{\partial x_0}\right)^{-1}\Big|_{A4} = C\delta(v_\infty - v_s) \qquad (13)$$

Using (10) and performing the integral in the A4 region we compute the value of C

$$C = \frac{\sqrt{2\alpha_v\alpha_T} - \xi_\infty}{\left(\alpha_v + \sqrt{2\alpha_v\alpha_T} - 1\right)\left(1 + \sqrt{2\alpha_v/\alpha_T}\right)} \qquad (14)$$

The additive contribution of region A4 into (7) is then

$$\left(\Delta f_{v_\infty}\right)_{A4} = f_{q/m}\left[\frac{q}{m}(v_\infty)\right] C\left[\frac{q}{m}(v_\infty)\right]\sqrt{2\frac{q}{m}\frac{1}{V}} \qquad (15)$$

If the spectrum of the measurement is known (known $f_{q/m}\left(q/m\right)$), then we can compute the integral in (7) directly to obtain the distribution function for the gate-leaving velocity $v_\infty$.

In the experimental results presented in [4], the working fluid was Tributyl Phosphate (TBP) doped with an ionic liquid. The dielectric constant of TBP solutions is relatively low, and therefore the specific charge is limited to low values. TOF measurements done by Gamero [5] for the same fluid yielded q/m values close to those predicted by the cone-jet electrospray theory of F. de la Mora [6]

$$\frac{q}{m} = \frac{I}{\rho Q} = \frac{f(\varepsilon)}{\rho}\sqrt{\frac{\gamma K}{\varepsilon Q}} \qquad (16)$$

For the experimental conditions used in [4] (shown in table 3) a q/m value of about 127 C/kg was expected, which corresponds to a time of flight of 355μsec.

Table 3 — Experimental parameters used in [4]

| Qty. | Value | Qty. | Value |
|---|---|---|---|
| $f(\varepsilon)$ | 7 | $T$ | $30\times10^{-6}$ s |
| $\varepsilon$ | 8.9 | $x_m$ | 10 mm |
| $\rho$ | 976 kg/m$^3$ | $x_\infty$ | 15 mm |
| $\gamma$ | 0.028 N/m | $V$ | 700 V |
| $K$ | 0.05 Si/m | $\phi_m$ | 950 V |
| $Q$ | $5\times10^{-13}$ m$^3$/s | $L_{drift}$ | 15 cm |

As shown in figure 2, for a specific charge of q/m = 127 C/kg, the velocity at the exit plane is modified for all particles, in particular all of them suffer a net acceleration which depends on the point they were located at the time the gate opened. The continuous line in figure 4 shows the experimental data from [4]. The theory predicted a peak near 355μsec. Instead, a broad peak appeared close to 260μsec, significantly faster than expected.

We can now perform the exercise of calculating the effect the gate has on a pure spectral line. Assume that we know the ideal distribution function for specific charge, and suppose that it has a single peak at q/m = 127 C/kg, in the same way as the expected experimental measurements of [4]. This function is shown as the finite width (Gaussian shaped) peak in figure 3.

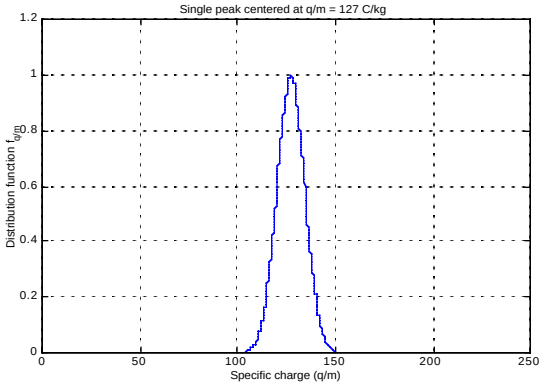


Figure 3 — Single peak at q/m = 127 C/kg

The velocity distribution function is computed directly from (7) and the result is shown as the dashed line in figure 4.

There are two important points that can be extracted from this calculation: (a) there is no evidence of the nominal peak at 355μsec, which is in agreement with the discussion above which lead to figure 2. And (b) the peak was shifted to higher velocities and broadened as predicted. It is also interesting to see that the calculated peak resembles the one that was obtained experimentally.

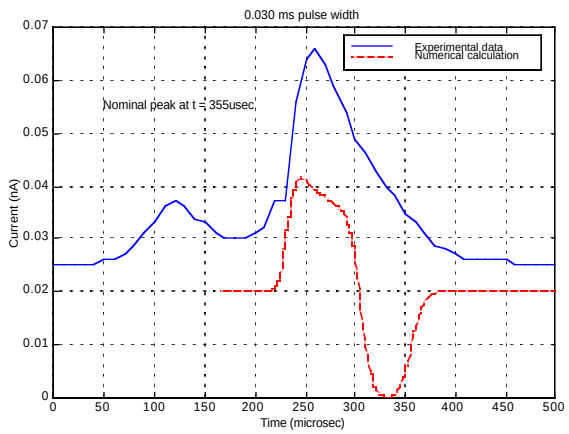


Figure 4 — Comparison of experimental data with results from the electrostatic gate model

This exercise is useful for verifying the assumptions made in the electrostatic gate model, but of course it would be much more interesting to solve the inverse problem: given the velocity distribution function (experimental data) obtain the specific charge distribution.

For this purpose, equation (7) can be viewed as Fredholm integral equation of the first kind for the unknown input spectrum $f_{q/m}$. Discretization of the quantities inside the integral symbol by using a numerical method, such as the trapezoidal rule

$$\int_a^b f(x)dx = \frac{h}{2}\left[ f(a) + f(b) + 2\sum_{k=1}^{n-1} f(x_k) \right] + \ldots \quad (17)$$

where $h = \frac{b-a}{n}$ and $x_k = a + kh$, allow us to write (7) as a matrix equation of the form

$$\dot{f}_{v_\infty} = \mathrm{K}\dot{f}_{q/m} \quad (18)$$

where **K** is commonly known as the equation kernel. In principle one could find the solution by inverting the kernel. However, for this kind of equations, the kernel is almost always singular to some degree and inversion by common methods usually fails.

Singular value decomposition (SVD) can be used to obtain an approximation to the matrix inverse in a least-squares sense. Since an exact solution is not possible, some information is always lost in the physical process triggered by the electrostatic gates.

If the kernel matrix **K** is square, then it can be decomposed in two unitary matrices **U** and **V** and a third diagonal matrix **W**

$$\mathrm{K} = \mathrm{U}\mathrm{W}\mathrm{V}^{\mathrm{T}} \quad (19)$$

The inverse of (19) can be easily computed, since the inverse of a unitary matrix is its transpose and the inverse of a diagonal matrix is also diagonal, formed by the reciprocals its elements,

$$\mathrm{K}^{-1} = \mathrm{V}\left[\mathrm{diag}\left(1/\mathrm{w}_{\mathrm{j}}\right)\right]\mathrm{U}^{\mathrm{T}} \quad (20)$$

The problem appears when some of these $w_j$'s are very small or zero. This implies that there is no physical process in the model that would yield a mode with such singular values and therefore they would contribute only to noise in the system. Information would be lost, as we predicted, if we remove them, but we must do so to be able to have a good approximation to the kernel inverse.

Applying this procedure to the experimental data obtained in [4] yields the result plotted in figure 5.

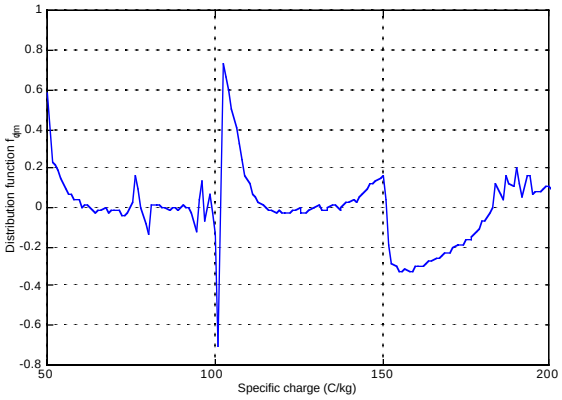


Figure 5 — Results from inverting the matrix

A prominent peak can be seen close to q/m = 102 C/kg. Not exactly the 127 C/kg that was expected theoretically, but by far closer to it than the value of 230 C/kg that can be estimated by only looking at the measured spectra.

This is encouraging in the sense that the method was able to recover some useful information from data taken in very adverse conditions; namely, when the velocity of all particles was modified by the effect of the electrostatic gate.

## Sensitivity of the gate effect

These results could be used to improve the design of an electrostatically gated spectrometer in two ways: (a) by recovering information from otherwise corrupted data, and (b) by assessing how modifications in the hardware parameters could modify the outcome of the measurement.

The first improvement was already discussed in the section above. For the second, we could try different combinations of parameters to see their effects on the distribution functions.

Two cases were analyzed, in the first one the distances between the gated electrode and the grounds were changed to half the size described in table 3 leaving everything else constant. The results of this are shown in figure 6.

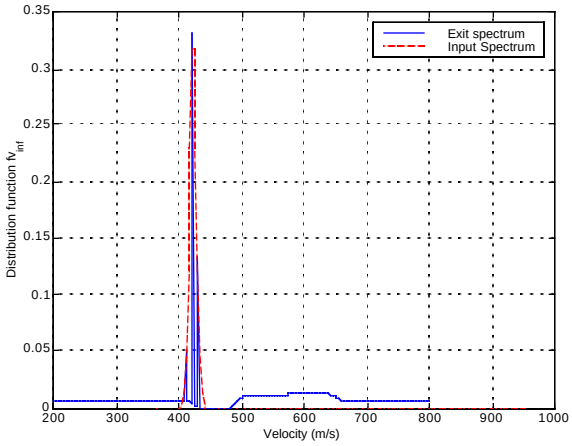


Figure 6 — Effect of geometry change in a single peak at q/m = 127 C/kg

This simple change decreases the time the particles spend inside the gate, and therefore some of them fall in region A4. Besides some distribution of particles at higher velocities, we can observe the appearance of a distinctive peak at about 420 m/s, corresponding to q/m = 127 C/kg.

In the second case two changes are made; the electrode's geometry is modified such that $x_m$ = 3mm and $x_\infty$ = 9mm and also the fluid is changed to one with higher q/m, like Formamide ($CH_3NO$) doped with NaI salt.

From de la Mora's theory [3] we compute q/m for a solution with $K$ = 2.32 Si/m, $\gamma$ = 0.058 N/m, $\rho$ = 1133.4 kg/m$^3$, $\varepsilon$ = 111, $f(\varepsilon)$ = 20 and $Q = 8.3\times10^{-13}$ m$^3$/s, from (16) we obtain q/m = 674 C/kg, which corresponds to a velocity of 1021 m/s if the acceleration potential is $V$ = 774 V. A time of flight of 154μsec is calculated if the drift distance between gates is $L_{drift}$ = 15.7 cm. The results of applying the model are shown in figure 7.

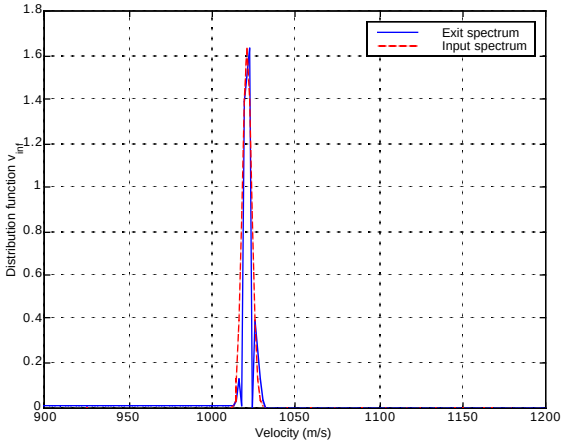


Figure 7 — Effect of fluid and geometry change (Formamide, q/m = 674 C/kg)

We can see that the effect of using a faster solution is similar to the one we obtained by reducing the size of the gate. Physically speaking both cases minimize the time the particles spend inside the gate, so the results are what we could expect.

## Experimental Results

To verify the second alternative presented above, experiments were performed using a Formamide solution with the same characteristics already described. The measurements are shown in figure 8, including error bars. In contrast with the results reported in [4], the peak observed near 160μsec agrees quite well with what can be expected from the electrospray theory. From our discussion above we determine that the finite-width gate effect is small enough to dramatically change the spectrum characteristics.

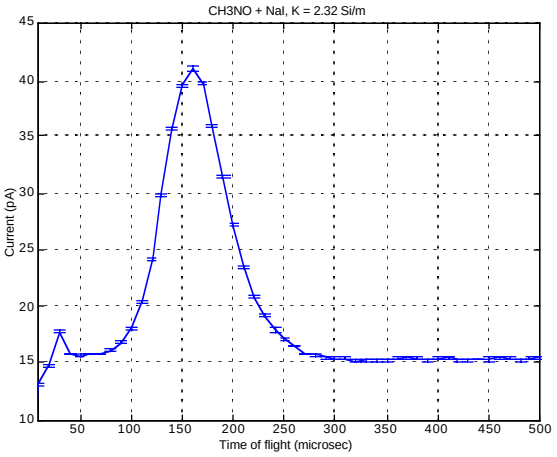


Figure 8 — Experimental results with Formamide

## Conclusions

A mathematical model for finite-width electrostatic gates was presented to analyze the effects that such devices have on TOF measurements for Colloid Thrusters. It was found that such gates introduce velocity variations, which are stronger for slow charged particles or for large gates. Zero-width gates are more difficult to work with since the micro interleaved comb assembly could get short circuited by liquid deposition. Deflection plates introduce other effects, among them a reduction of the current measured. The electrostatic gate model was used also to recover useful information from degraded data. A new set of experimental results showed that model predictions are accurate and that they could be used to design TOF hardware.

## References

[1] M. Martinez-Sanchez, J. Fernandez de la Mora, V. Hruby, M. Gamero-Castaño and V. Khayms, *Research on Colloid Thrusters.* Paper IEPC 99-014, 26th IEPC Kitakyushu, Japan, Oct. 1999.

[2] J. Perel, T. Bates, J. Mahoney, R.D. Moore, *Research on a charged Particle Bipolar Thruster.* Paper No. 67-728, AIAA Electric Propulsion and Plasma Dynamics Conference, Colorado Springs, CO, September 1967

[3] M. Gamero-Castaño, private communication (April 2001)

[4] P. Lozano, M. Martinez-Sanchez, *Experimental Study of Colloid Plumes,* 37th JPC, Salt Lake City, Utah, AIAA 2001-3334

[5] M. Gamero-Castaño and V. Hruby, *Electric Measurements of Charged Sprays Emitted by Cone-Jets,* New York: Submitted for publication.

[6] J. Fernandez de la Mora, *The Current Emitted by Highly Conducting Taylor Cones.* J. Fluid Mech. (1994), Vol. 260, pp. 155-184